Instability of Charge Qubit Outfitted in a Double Quantum Dot

I. Filikhin[1], A. Karoui[1], V. Mitic[2], T. Zatezalo[1], and B. Vlahovic[1]

[1] CREST/Mathematics and Physics Department, North Carolina Central University, Durham, NC 27707 USA

[2] University of Nis, Faculty of Electronic Engineering, Nis, Serbia, and University of Belgrade, Institute of Technical Sciences, Serbian Academy of Sciences and Arts, Belgrade, Serbia

e-mail: ifilikhin@nccu.edu

Abstract. We study electron tunneling in binary quantum systems as double quantum dot (DQD) and double quantum well (DQW), considered as two-level systems. The Schrödinger equation for this system is reduced using single band $\boldsymbol{kp}$-effective Hamiltonian, and is solved numerically. We calculate full electron spectrum E_n, $n = 1, 2 \dots$ in the bi-confinement potential. The tunneling in DQD is studied in relation to two factors, a coupling coefficient W_n and an asymmetry factor Δ_n of the potential. The ratio W_n/Δ_n defines the electron localization in DQD. The cases of ideal and almost ideal DQD are examined and compared. We are modeling the effects of environmental influence and fluctuations of electrical pulse on the coherence of DQD based charge qubit. In particular, we show that the coupling in the ideal DQD (Δ_n=0) is unstable for any small fluctuations of Δ_n.

Keywords: Electron tunneling, Electron localization, Quantum wells, Semiconductors, Electric field, Charge qubit

PACS numbers: 73.20.Dx,73.43.Jn,73.21.Fg,73.21.La,78.67.-n,03.67.Lx

1. Introduction

Semiconductor solid-state structures were and are promising for building quantum computers. Since Loss and DiVincenzo's proposal in Ref. [1] an electron spin qubit in quantum dots in 1998, the quantum computers have been realized by different physical principles. One of them is the concept of a spatial isolating single electron in double quantum dots (DQDs) [2, 3]. The electrically gated quantum dots in semiconductor heterostructures are attractive for quantum computations because produce qubits that are simpler manipulability, scalability, and interactively with classical electronics. Such GaAs quantum dot system with one- and two-qubit devices have been experimentally demonstrated in Ref. [4, 5, 6]. The charge qubit based on electron localization in a left or right quantum dot of a DQD has been proposed in Refs. [7, 8, 9] and [10]. The control is achieved by capacitively coupled elements like gates for state initialization and modification, and single-electron transistor for measuring tunneling current. The theoretical description for Si/SiGe and graphene DQD based qubits can be found in Refs. [10, 11, 12].

One of the main problems with quantum computing is the qubit error induction. The quantum states of qubits are indeed sensitive to slight variations of temperature or tiny vibration, and even single stray photons. These can cause random qubit's state change, which gives rise to non-controllable error. The state of neighboring qubits can also change haphazardly as a QD can pick up signals intended for their neighbors. The quantum fluctuations or "charge noise" on a controlled phase gate may perturb the charge stability in a substantial way [13, 14, 15]. In addition, symmetry breaking has also a crucial issue in quantum engineering since it causes coupling of quantum states of QDs [16].

Our goal is to explore the importance of symmetry on the stability of qubits. To that end, we propose an original approach to describe the electron tunneling based on electron states modeled using the entire electron confinement spectrum. The theoretical description for InAs/GaAs heterostructures is based on the effective potential model proposed in Ref. [17]. Main aspects of symmetry violation and how each affects the entanglement were studied in Refs. [18, 19, 20, 21, 22, 23, 24]. In line with this study, we evaluate how small variations of the system geometrical parameters (QD size and shape, and the DQD topology) and applied fields will affect the stability of localized/delocalized states in DQD. Other external factors and conditions that may affect the qubit are not considered in this paper (e.g., emission or absorption of photons and phonons). Also, we delineate the limits at which charge tunneling in ideal DQD becomes unstable with small fluctuations affecting the whole spectrum of the electron confinement. We assert that ideal DQD (defined as a system with infinite coherence) systematically becomes unstable under any small level of fluctuation, a feature that turns a DQD into an extremely sensitive sensor, as proposed in our paper [18].

In the present paper, we focus on two types of charge qubit effectors: the environment, which distorts the wave function of an electron in coupled DQD, and

fluctuations induced by an electrical pulse. Fluctuation risers (for instance, a molecule that is being detected) change the coupling parameter W and asymmetry Δ of bi-confinement in DQD. Our numerical modeling is related to analysis for dynamics of localized/delocalized states in electron spectrum under DQD geometry variations. We demonstrate that the ratio W/Δ controls the electron localization in DQD. The modeling of the variations of the geometry allows us to simulate the effects of environmental influence and fluctuations of electrical pulse on the coherence in the DQD based charge qubit. We show that the numerical uncertainty like 0/0 takes place and defines the spectral distribution of localized/delocalized states in an ideal DQD (Δ =0). Such ideal systems are appropriate for theoretical description when the mathematical limit $\Delta \to 0$ is possible. In this paper, we consider realistic binary quantum systems.

This paper is organized as follows. In Section 2 our theoretical model of InAs/GaAs heterostructures for quantum dots is presented. In Section 3 theoretical discussion of two-level systems, anti-crossing levels, and electron coupling in double quantum dots are given. To illustrate the theory, the results of our calculations for the electron tunneling in DQD induced by an external electric field are presented in Sec. 4. Section 5 discusses numerical examples of distributions of localized and delocalized states in the spectrum of a single electron and the influence of numerical and geometry factors on the tunneling for two cases, the ideal and "non-ideal" symmetric in double quantum well. An interpretation of the results is presented in Sec. 6. We describe the spectral instability of DQD tunneling with the effects of environmental influence and fluctuations of electrical pulse on the coherence of DQD based charge qubit. Concluding remarks are provided in Sec. 7.

2. Model

The electron state in InAs/GaAs QDs is modeled [17] based on the kp-perturbation single sub-band effective mass approximation. In this case, the eigenvalue problem is formulated by the Schrödinger equation:

$$\left(\widehat{H}_{kp} + V_c(r) + V_s r \right) \Psi(r) = E \Psi(r), \tag{1}$$

where E is the electron binding energy, $\widehat{H}_{kp}$ is the single band **kp**-Hamiltonian operator $\widehat{H}_{kp} = -\nabla \frac{\hbar^2}{2m^*} \nabla$, m^* is the electron effective mass, which depends on the radial position of the electron, thus can be written as $m^*(r)$, and $V_c(r)$ is the band gap potential. The Ben-Daniel-Duke boundary conditions [25] are used at the interface of the QW material and the substrate. Here, we describe the confinement model proposed in Ref. [17] for the conduction band. Both potentials $V_c(r)$ and $V_s(r)$ act within the QWs extent. While the potential V_c is attractive, the potential V_s is repulsive. The V_s potential reduces the strength of the electron confinement; it is added to simulate the strain effect in the InAs/GaAs heterostructure.

The energy is measured so that inside the QD the bulk conduction band offset is null, i.e., $V_c = 0$, while it is equal to V_c outside the QD. The band gap potential for the conduction band is fixed to $V_c(r) = 0.594$ eV. The bulk effective masses of InAs and GaAs are $m_1^* = 0.024\ m_0$ and $m_2^* = 0.067\ m_0$, respectively, where m_0 is the free electron mass.

The magnitude of the effective potential $V_s(r)$ that simulates the strain effect is adjusted so to reproduce experimental data for the InAs/GaAs quantum dots. The adjustment depends mainly on the materials composing the heterojunction, and to a lesser degree, on the QD topology. For example, the magnitude of $V_s = 0.21\ eV$ for the conduction band was discussed in Ref. [17]. This value was adopted as it reproduces results obtained based on eighth band $\boldsymbol{kp}$-calculations for InAs/GaAs QDs [26]. Another value of 0.31 eV for V_s was obtained [27] from experimental data reported by Lorke et al. [28]. The main advantage of using the effective potential is the theoretical simplicity, as well as the practical calculations, even in the case of complex geometry of nano-sized systems.

The model is compatible with existing experimental data for InAs/GaAs heterostructures. For example, in Ref. [29], an interpretation of the C–V data has been proposed and compared to Lei et al. study [30] given on the basis of oscillator model for quantum ring (QR). Two sets of geometry parameters for self-assembled QR were used. The first is from a QR experimental prototype and the second from the oscillator model matching the model parameters, including the size of the quantum objects. The additional energy of an electron in a magnetic field was calculated with both QR geometries. It has been shown that the results of the calculation with the second geometry fit the C–V experimental data rather well.

3. DQD as a two-level system

We consider two coupled InAs/GaAs quantum dots as an example of a two-level system. The confinement of an electron is modeled by one dimensional formalism which can be found in Ref. [31]. In the ($|0\rangle$, $|1\rangle$) basis of electron state in separated quantum dot pair, the Hamiltonian (1) takes the matrix form:

$$H = \begin{pmatrix} E_1 & W \\ W & E_2 \end{pmatrix}. \tag{2}$$

At that the wave function of an electron state is written as the superposition $\alpha|0\rangle + \beta|1\rangle$. By diagonalizing the matrix (2), the electron single-particle energies are calculated [31] as

$$E_+, E_- = \frac{(E_1 + E_2) \pm \sqrt{(E_1 - E_2)^2 + 4W^2}}{2}.$$

In the absence of the tunnel coupling, i.e., at $W = 0$, the two dots are independent, and these energies are simply equal to the lower and the higher of the two energies

E_+, E_-, respectively. Here, $W > 0$ and the coupling W exists due to overlapping wave functions of the undisturbed state of two separated QDs having the energies E_1, E_2. When the energy difference $\Delta = |E_1 - E_2|$ is large, no tunneling occurs. The maximal tunneling corresponds to the value $\Delta = 0$ with energy gap ε. The energy diagram in Fig. 1 clarifies this setting. For non-identical QDs in DQD, the main factor for tunneling, which defines the coupled strength W, is the inter-dot distance. Other factors include the spatial configuration of the wave function, which depends on generalized quantum numbers, such as the radial quantum number and orbital momentum. In Ref. [18], it was shown for identical QDs in DQD, that the uncertainty of type $0/0$ for some confinement levels of the electron spectrum takes place in numerical analysis. That reflects the instability of spectral distribution of localized/delocalized states of identical QDs relative the small deviations of QDs geometry and inter-dot distances (see Ref. [18]). For DQD with an asymmetric geometry, the main factor for tunneling sensitivity is the inter-dot distance. For small distances, the value W can be essentially large so to provide a stable tunneling. Here, we assume similarity of geometry of QDs in DQD. The tunneling stimulated in DQD having a defect in one of the two QDs, which violate the symmetry, leads to instability.
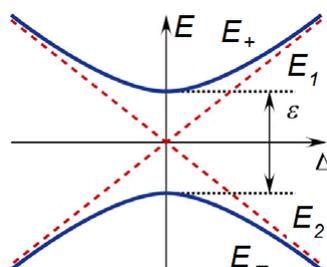
Figure 1: The anti-crossing in a two-level system as dependence of the energy of levels, E_+, E_-, (solid curves) on the deference Δ of energies E_1, E_2, of the corresponding levels for uncoupled system (red dashed lines).

4   Electron tunneling in double quantum dots in electric field

Considering laterally distributed 3D DQD in an perpendicular electric field, we varied the geometry parameters and values of electric field to replicate the anti-crossing of levels that has experimentally evidenced. The results of our modeling are presented in Fig. 2. Here, the Stark effect results in level anti-crossing at 2.5 kV/cm. As shown, the electron is transferred from one QD to another one as the electric field is changed from zero to a value larger than 2.5 kV/cm. Note, that the anti-crossing is taking a place for a finite value of Δ, the asymmetry factor due to non-identical QDs in the DQD.
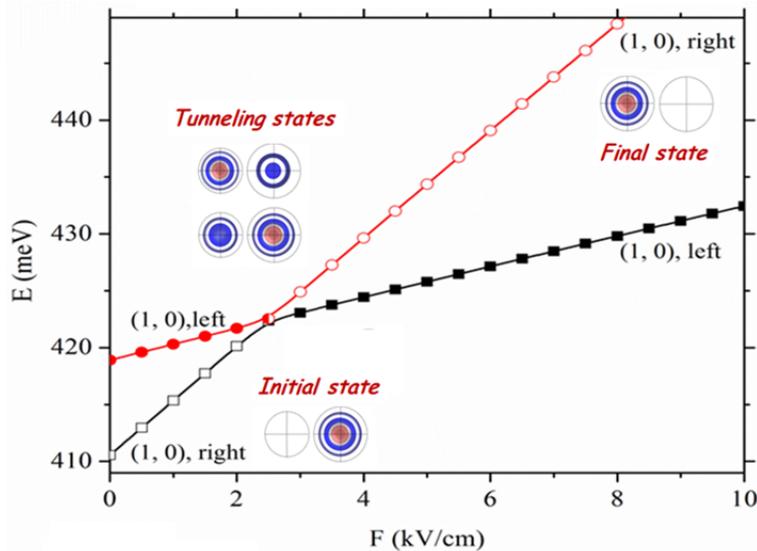
Figure 2: Anti-crossing of levels in InAs/GaAs DQD controlled by the electric field. The diameters of the spherical cap shaped quantum dots QD_1 and QD_2 in the cut plan are D_1=38 nm and D_2=34 nm, respectively. Their height is H=8 nm, while the inter-dot distance is a=3 nm. The electric field magnitude is denoted F, and the energy of an electron in the DQD is E (Insets). The square of the wave function is shown for initial, tunneling and final states.

One must note that the electron localization in the tunneling state depends on geometry and material parameters of the QDs. The case of a localization described by ideal relation $(1/2\ |L\rangle^2 + 1/2\ |R\rangle^2)$, where $|L\rangle$ and $|R\rangle$ are the electron wave functions in the "initial" state with no external field ($F = 0$), is not experimentally achievable. The $(\alpha\ |L\rangle^2 + \beta\ |R\rangle^2)$ relation is accurate and more realistic. Hence, the stability of the DQD based qubit depends on ratio α/β. If that ratio is small or very large (relative to 1), the qubit stability is weak compared to that of a qubit on ideal DQD, in which case the ratio $\alpha/\beta\ = 1$. Ideally, the QDs must have exactly the same geometry and material properties for a maximum coherence; such system is expected to uphold a longer coherence.

5. Electron tunneling in double quantum wells

We present a numerical model for charge qubit made of InAs/GaAs double quantum dot, allowing a detailed analysis of the electron localization and spectral distributions of localized/delocalized states. Note that an experimental technique for registration of the excited states in DQD has been proposed in Ref. [32], the authors used capacitive charge sensing to single out such states. It was shown in Ref. [18], that the electron tunneling and spectral distributions of localized/delocalized states in this binary system are extremely sensitive to the shape symmetry viola-

tion. We consider electron levels in bi-confinement potential with the energies E_n, $n = 1, 2, 3 \ldots$ listed in increased order of energy values. The model utilizes QD coupling parameter, namely Θ, which defines the delocalized ($\Theta \approx \frac{\pi}{2}$) and localized ($\Theta \approx 0$) states of electrons. This parameter depends on Δ_n, the difference between energy levels of the left and right QDs, the considered spectra are those of separated QDs. The difference can be caused by a shape symmetry violation. For one-dimensional two-level system, the dependence of the localization of a single electron in DQD may be presented [31] by a simple function of the ratio W_n/Δ_n, where W_n is defined by overlapping the wave functions of separated QDs and Δ_n is the energy difference between n-th electron levels in the spectra of separated QDs:

$$\Theta = \arctan(2W_n/\Delta_n), \ n = 1, 2, 3, \ \ldots. \tag{3}$$

The dependence of Θ on the dissymmetry ratio is shown in Fig. 3. Here, the "delocalized state" demonstrates the coupling of the QWs. The wave functions of each quasi-doublet can be expressed as follows:

$$\Psi_+ = \psi_1 + \tan(\Theta/2)\psi_2, \qquad \Psi_- = -\tan(\Theta/2)\psi_1 + \psi_2$$

with accuracy on normalizing constant. Where the "unperturbed states" ψ_1 and ψ_2 of separated left (index 1) and right (index 2) quantum wells are notated.
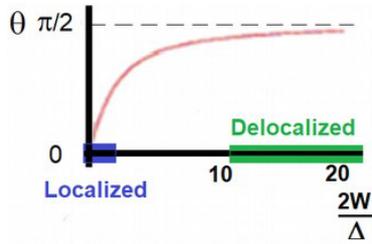
Figure 3: The localization of single electron in DQW: the relation between the coupling parameter Θ and the ratio $2W/\Delta$ for a confinement level in DQW is given. We show the ranges for localized and delocalized states of the electron in DQW.

To evaluate the electron localization, we analyze the single electron average coordinate $\langle x \rangle$, calculated as the matrix elements $\langle x \rangle_i = \langle i | \ x \ | i \rangle$ for $i=1$, 2, ($\langle x \rangle_{ij} = \langle i | \ x \ | j \rangle$) which are associated, respectively, with the electron wave functions in QW$_1$ and QW$_2$, considered separated. The origin of the x-coordinate is chosen to be the mid-point of the two QWs. The average coordinate $\langle x \rangle_+$ and $\langle x \rangle_-$ can be written as:

$$\langle x \rangle_+ = \langle x \rangle_1 + \tan^2(\Theta/2)\langle x \rangle_2 + 2\tan(\Theta/2)\langle x \rangle_{12}$$

and

$$\langle x \rangle_- = \tan^2(\Theta/2) \ \langle x \rangle_1 + \langle x \rangle_2 - 2\tan(\Theta/2)\langle x \rangle_{12}$$

for corresponding quasi-doublets of the electron spectrum.

The sensitivity of the parameter Θ to small variations of Δ and W is estimated [18] as:

$$\delta(\Theta) \sim -\frac{W}{\Delta^2 + W^2}\delta(\Delta) + \frac{\Delta}{\Delta^2 + W^2}\delta(W), \tag{4}$$

where W and Δ depend on the quantum number, they are selected from W_n and Δ_n.

Below we present a numerical analysis for the electron tunneling in InAs/GaAs of a typical double quantum well modeled using the above discussed material parameters, separately with either identical QWs (ideal DQW) or non-identical QWs but almost ideal DQW. The chosen geometry of the DQW is motivated by experimental fabrication given in Ref. [33]. This DQW is made basically of ellipsoidal dots, as presented in Fig. 4. It has been demonstrated in Ref. [18], that small variations of dot geometry violating the symmetry in DQD disturb essentially the spectral distribution picture for the tunneling states and electron confinement.
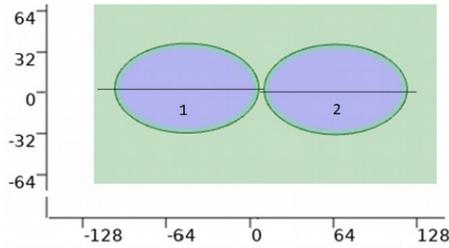
Figure 4: Utilized geometry of ellipsoidal DQW: The size of QW_1 and QW_2 are determined by the semi-axis R_1=55nm, R_2=34.75 nm, and the vertical gap s=1 nm in asymmetric case. The geometry is motivated by experimental data from fabricated double quantum dot complexes from Ref.[33].

Therefore, the geometry deviation between the two cases is considered as a key parameter; the symmetry violation occurs even by miniscule geometry difference of the second dot of the DQW relative to the first. The results of the calculations are shown in Fig. 5. We found that the quantum behaviors of the two cases are fundamentally different. The tunneling spectral distribution for the asymmetric DQW (see Fig. 5b)) case has a complex character. The electron delocalization appears to depend on the size of the bridge connecting the two QWs and the QW size difference. The localized states are dominating in the electron energy spectrum. Conversely, the spectral distribution for the symmetric DQW is simple; all states in the symmetric DQW spectrum are delocalized. However, the limitation of numerical calculations does not unravel this simplistic case directly.

In Fig. 5 (a), the localized/delocalized states are shown for three different meshes used for solving numerically the Schrödinger equation, needed for the finite element analysis (FEA) solver. The mesh sizes were chosen to be fine up to full extent of the available computer memory (32GB) and to the limit of software capabilities in terms of nodes. The finest mesh (Mesh 3) appeared to provide larger delocalizing (tunneling states). The energy spectrum of single electron can be sorted according to electron localization probability. As a result, a set of localized states (in the left QW or right QW) appear either at around $\langle x \rangle \approx \pm maxj\langle x \rangle j$, or around $\langle x \rangle \sim 0$ (delocalized states), or in between where states have different probabilities of being in the left and right QWs. The Mesh3 results (purple-colored dots) are essentially clustered around $\langle x \rangle = 0$ location. This means that delocalized states become dominated. The finalized result can be obtained by unlimited decrease of the mesh cell size. Such decrease is not possible to be manage numerically based on finite difference methods.

The ideal case corresponds to total delocalized spectrum conducive to electron

confinement states in DQW. It is clear that this situation cannot be experimentally reproduced. We should note that in the literature (see Ref. [34, 35] for an example) the theoretical analysis has been limited to the ideal case.

The calculation for asymmetric DQW shown in Fig. 5b) is numerically more stable, converges more rapidly, and the mesh variations affect mostly the energy of states located near the threshold of the confinement in the QW. The calculation is supported with the mesh refinement. The contrast between ideally symmetric DQW and asymmetric one is the strong dependence of the tunneling on inter-dot (well) distance. For ideal case, the inter-dot distance is irrelevant as it does not affect the tunneling. In the case with violated symmetry, the distance plays significant role as it hinders and even blocks the electron tunneling.

For the numerical modeling of the ellipsoidal DQWs with increasing asymmetry, we used two sets of geometry parameters. For the first set, QW1 has a semi-axis ratio of R_1/R_2=55/35 and the QW2 has a ratio of R_1/R_2=55/34.90; the relative shift along the horizontal axis is s=1 nm. The second set has the same geometrical parameters for QW1, but for QW2 the parameters are chosen to be: R_1/R_2=55/34.75 and s=-2 nm. The first set is closest to symmetric DQW. The results of calculations are given in Fig. 6, where in a) the first DQW (the closest to the ideal case) corresponds to more delocalized states in the spectrum than the second DQW with larger geometry difference. The energy difference Δ of the spectra of the separated QWs for these two variants of QDW geometry is presented in Fig. 6b). One can conclude that the tunneling in the DQW is a concurrent effect of complex interplay between W_n and Δ_n, both convey the dissymmetry of the two QDs. However,
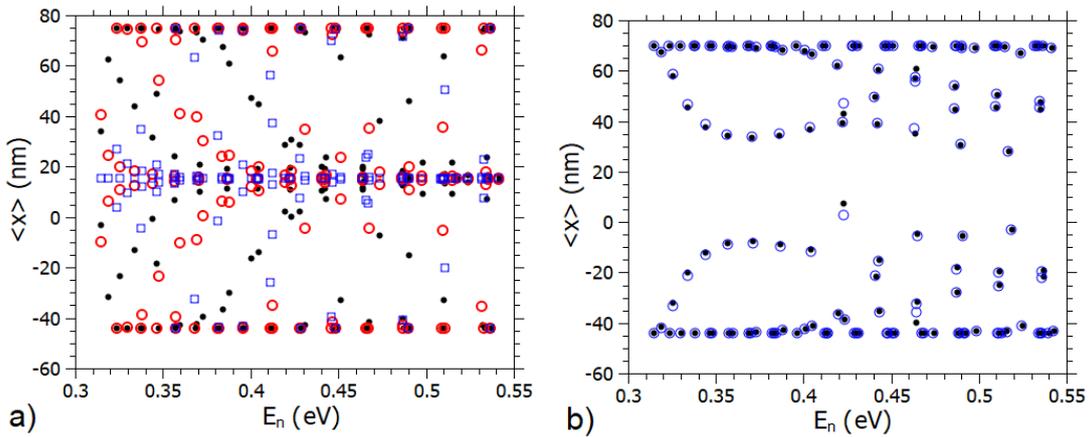
Figure 5: (a) The "ideal" DQW: the tunneling in symmetric ellipsoidal DQW: the sizes of QW$_1$ and QW$_2$ are equal. The results of calculation for different three meshes are shown by dots (Fine mesh), open circles (Finer mesh), and open rectangles (Finest mesh). (b) The tunneling in "almost ideal" DQW: asymmetric ellipsoidal dots (size of QW$_1$(R_1/R_2 = 55/35)) is larger than the size of QW$_2$(R_1/R_2 = 55/34.75). The QW horizontal axes are shifted by s=1 nm. Open and close circles show the results related to the mesh variations.
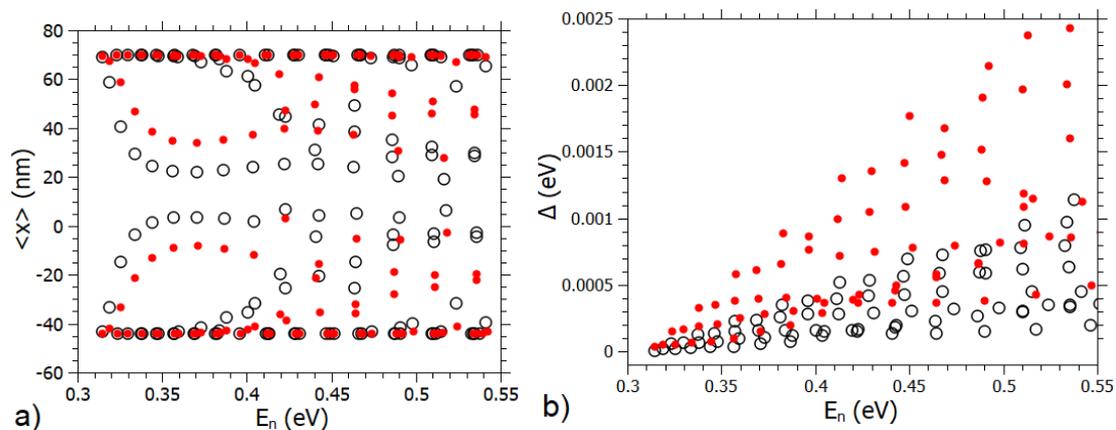
Figure 6: a) The tunneling in ellipsoidal DQW with two set geometry parameters with increasing asymmetry of the DQW. The solid circles are related to the first DQW (the set where $R_1/R_2 = 55/34.75$ and s=1 nm for QW2). The open circles are for the second DQW (the set where R_1/R_2=55/34.90 and s=-2 nm for QW2). b) The energy asymmetry Δ of the spectra of the separated QWs for these two variants of QDW geometry.

this numerical experiment demonstrates that small variations Δ_n can drastically affect the tunneling. The "traces" which are visible in Fig. 6a) can be interpreted as a separation of the values $2W_n/\Delta_n$ according to the spatial symmetries of corresponding wave functions.

The data presented in Fig. 5 can be also described in terms of regular (ideal DQW) and chaotic (asymmetric DQW) behavior for tunneling rate in binary quantum well, reported in Ref. [21]. The effect of transformation of double quantum well geometry from "regular" one to "chaotic" on the tunneling rate along the energy spectrum is demonstrated through this data. The electron spectrum of coupled QWs is formed by a set of quasi-doublets, according to Eq. (2). Evaluation of quasi-doublet energy splitting ε is performed using the formula:

$$\varepsilon \sim \int \Psi_{\mathrm{sL}}(x,\ y)V\ (x,\ y)\Psi_{\mathrm{sR}}(x,\ y)dxdy,$$

where $\Psi_{\mathrm{sL}}(x,y)$ (resp. $\Psi_{\mathrm{sR}}(x,y)$) is the normalized wave function of the "single left" (resp. "single right") QW. The result of the integration depends on overlapping of the wave functions. The parameters that define this overlapping integral are the distance between QWs and the spillover of the single wave function outside of the QW shape region, which depends on the energy of the considered level. The wave function spread is due to the asymptotic behavior of the confined states. Such asymptotic behavior is written as: $\Psi(x) \sim A exp(-b\ \sqrt{E_c - E}\ x)$, where x is the distance from a QW boundary, A and b are constants (at most, they would depend on an quantum numbers (like to orbital numbers), see regular located "traces" in Figs. 5b)-6, E_c is the threshold of the continuous spectrum. It can be shown that the value of logarithm of the tunneling rate $\ln(\varepsilon)$ depends on the energy as a linear

function of $\sqrt{E}$. The tunneling rate ε is correlated to the coupling coefficient W_n.

6.   On the instability of charge qubit based on double quantum dot

Based on our approaches and related findings, we propose a new interpretation for the spectral instability of DQD tunneling. This new picture is relevant to quantum computing, as it unravels instability of tunneling in qubits under certain conditions and proposes solution to overcome (or minimize) the effects of the instability. The charge qubit can be characterized by a bi-stable potential, which is in line with published data in Refs. [7, 36, 37, 38, 39, 40, 41] it allows for not only separation of states based on energy, but also on spatial separation, as well as on localization of states in different potential wells (i.e., individual/separate QDs). We have shown in previous sections that the tunneling in a two-level system, exactly like in the DQD, is extremely sensitive to fluctuations, as described in Eq. (3) and resulted by a concurrent effect of Δ and W. Thus, the tunneling in a DQD based qubit would be affected by any fluctuation of Δ and variation of W, both lead to loss of "coherency" of the qubit or "tunneling state" arising in DQD systems.

The ideal qubit is defined onto a DQD where the probability for an electron to be in the left QD or in the right is about 1/2 for all possible states of the DQD. This qubit state corresponds to the limits $\Delta \to 0$ and $W > \Delta$; these occur in a range of $\Theta \sim 0$, where the relation $tan(\Theta/2) \sim 1$ and the probability is close to 1/2. The limit $\Delta \to 0$ is a mathematical idealization, for which the spectral distribution of tunneling states in such ideal DQD corresponds to maximal qubit coherence. Nonetheless, the system remains unstable relatively to small fluctuations. This conclusion flows down from the results of our calculations, where the numerical errors simulate the small variations of input parameters of the almost ideal DQD.

More realistic consideration is conceived for finite values of Δ. A simple case to mention is when $\Delta \neq 0$ is induced by a geometrical asymmetry in DQD. To provide large value for the ratio W/Δ and stable tunneling, the value W has to be large so that $W > \Delta$ is always verified. For the asymmetrical DQD geometry or asymmetrical bi-confinement, it requests closely located the QDs in DQD.

The DQD based charge qubit is stimulated by an electrical pulse [7] which leads the tunneling in DQD to occur between the QD energy levels (considering the spectrum of initially decoupled QDs). For fabricated DQD, the energy difference Δ of initial state of the spectra is unrecoverable and this state can be a localized state, which might be caused by, for example, a relatively large inter-dot distance. This realistic situation is schematically illustrated in Fig. 7; where in a) there is no tunneling and the separated QDs energy levels are shown. During the pulse, the bias of the confinement potentials takes a place, as shown in Fig. 7b), which enables electron tunneling. The form of the fast electric pulse can be found in

Ref. [7]. The bias led tunneling in the DQD is due to the energy asymmetry Δ'; it is enabled as Δ' gets smaller than Δ. In this model, we assume that the pulse acts on the QDs in a non-adiabatic way. We demonstrated that the DQD
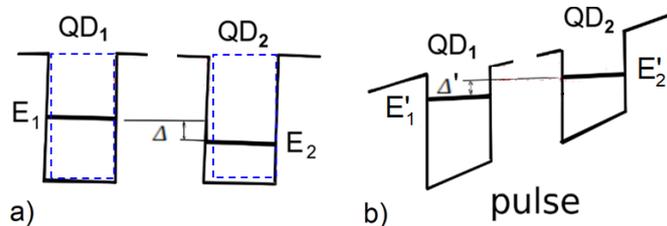
Figure 7: The confinement states of the single electron in separated QDs without (a) and with electrical pulse (b). Here, $\Delta' < \Delta$ due to the bias of the confinement potential in the electrical field. The fine dashed contour demonstrates non-similarity of the QDs.

state with the energy differences $\Delta' = 0$ is unstable relative to fluctuations and cannot be realized practically. We consider the situation, when $\Delta' < \Delta$. In this case, the above-mentioned concurrent effects of Δ and W take place. The effect of electrical field fluctuations during the pulse can give the different causal values for Δ'. The environmental induced fluctuations are mainly related to W. The environment media distorts the wave functions and changes the matrix elements. The complex competition of the two factors Δ and W demonstrated in Figs. 5 and 6, where results of numerical calculation simulate the interplay between Δ and W for different symmetry of wave functions and asymmetry of the bi-confinement (see, also Eq. (4). We can conclude that this interplay is a source of instability for the charge qubits.

The effects of fluctuations of the pulse have been formalized in Refs. [42, 43, 44], where the dephasing of a superconductor qubit was investigated. The wave function taking into account the dephasing can be represented by the formula:

$$|0\rangle + \beta e^{i\phi(t)}|1\rangle,$$

where the pre-factor of the $e^{i\varphi(t)}$ phase term can be described by a Gaussian distribution that expresses the fluctuations. Our analysis is in agreement with this phenomenological formalization. Additionally, we have to note that chaotic behavior of energy differences in the fluctuations is well described by the Wigner-Dyson spectral statistics [22, 23] (neighbor statistics). The DQD with realistic asymmetry is an example of such chaotic system.

7.   Conclusions

We have presented a basic model related to electron tunneling in DQD, an excellent device for making a charge qubit. The electron spin, if taken into consideration,

would lead to a more complicated picture of the anti-crossing levels [45, 46]. The spectral distribution of localized/delocalized states of the almost ideal DQD can be used for the interpretation of the instability of the qubit under environmental influence. We showed that the ratio W_n/Δ_n determinates the coherence in DQD; W_n is defined by the wave functions overlap for separated QDs and Δ_n is energy difference for the n-th electron level in the spectra of the separated QDs. The charge-based qubit was modeled numerically using two-dimensional (2D) and 3D binary systems with the quantum dots having different geometries. The concurrent effects of W_n and Δ_n and their contribution to the confinement spectrum is demonstrated by varying the DQD geometry. We found that the environmental fluctuations affect the symmetry of bi-confinement in DQD and can result in fluctuations of overlapping integral W_n and the energy shift Δ_n. Also, electric pulse fluctuations can result in variations of the energy shift Δ_n. Thus, the analyzed sources of the charge qubit instability clarify the usage range of the DQD for such an important application. The 2D DQD demonstrates high sensitivity to the DQD geometry variations. Our study clarifies ways for controlling DQD in practice for qubit application.

References

[1] Loss D. and DiVincenzo D. P.,Phys. Rev. A 1998, **57**, 120

[2] Elzerman J. M., *et al.* Phys. Rev. B 2003, **67**, 161308

[3] Ciorga M., *et al.* Phys. Rev. B 2000, **61**, R16315.

[4] Koppens F. H. L., Buizert C., Tielrooij K. J., Vink I. T., Nowack K. C., Meunier T., Kouwenhoven L. P. and Vandersypen L. M. K. Nature (London) 2006, **442**, 766

[5] Petta J. R., Johnson A. C., Marcus C. M., Hanson M. P. and Gossard A. C., Phys. Rev. Lett. 2004, **93**, 186802

[6] Oosterkamp T., Fujisawa T., van der Wiel W. *et al. Nature* 1998, **395**, 873

[7] Gorman J., Hasko D. G. and Williams D. A. Phys. Rev. Lett. 2005, **95**, 090502

[8] Simmons C. B. *at al.* Nano Letters 2009, **9**, 93234

[9] Sarma S. D., Wang X. and Yang Sh. Phys. Rev. B 2011, **83**, 235314

[10] Taranko R., Kwapiński T. Physica E 2013, **48**, 157

[11] Martin Raith M. *at al.*Phys. Rev. B 2014, **89**, 085414

[12] Hayashi T., Fujisawa T., Cheong H. D. et al. *Phys. Rev. Lett.* 2003, **91**, 226804/1

[13] Wang X., Yang Sh. and Sarma S. D. Phys. Rev. B 2011, **84**, 115301

[14] Yang S. and Sarma S. D. Phys. Rev. B 2011, **84**, 121306(R)

[15] Pan L., Wang X., Cui X. and Chen Sh. Phys. Rev. A 2020, **102**, 023306

[16] Yi, Yang S. arXiv:1912.05495v1 [cond-mat.str-el]

[17] Filikhin I., Suslov V. M., Vlahovic B. Phys. Rev. B 2006 **73**, 205332

[18] Filikhin I., Karoui A. and Vlahovic B. Journal of Nanotechnology, 2016, Vol. **2016**, Article ID 3794109

[19] Filikhin I., Matinyan S. G., Vlahovic B. Quantum Matter 2014, **3**, 549

[20] Filikhin I., Karoui A., Mitic V., Maswadeh W. and Vlahovic B., Res. J Opt. Photonics 2018, **2** , 2

[21] Filikhin I., Matinyan S G and Vlahovic B Sensors & Transducers 2014, **183**, 116

[22] Filikhin I., Matinyan S G and Vlahovic BPhys. Lett. A 2011, **375**, 620

[23] Filikhin I., Matinyan S. G., Schmid B. K. and Vlahovic B.Physica E 2010, **42**, 1979

[24] Filikhin I., Karoui A. and Vlahovic B. Int. J. Modern Phys. B 2016, **30**, 1642011

[25] Ben-Daniel D. J., Duke C. B. Phys. Rev. 1966, **152**, 683

[26] Schliwa A., Winkelnkemper M. and Bimberg D. Phys. Rev. B 2007, **76**, 205324

[27] Filikhin I., Suslov V. M., Wu M., Vlahovic B. Physica E 2009, **41**, 1358

[28] Lorke A., Luyken R. J., Govorov A. O. and Kotthaus J. P. Phys. Rev. Lett. 2000, **84**, 22236

[29] Filikhin I., Suslov V. M., Vlahovic B. J. Comp. and Theor. Nanoscience 2012, **9**, 669

[30] Lei W. *et al.* Appl. Phys. Lett. 2010, **96**, 033111

[31] Cohen-Tannoudji C., Diu B. and Laloe F. *Quantum Mechanics*, Vol. 1, 1977, Wiley-VCH, Weinheim, Germany

[32] Johnson A. C., Marcus C. M., Hanson M. P. and Gossard A. C. Phys. Rev. B 2005, **71**, 115333

[33] Wang Z. M., Holmes K, Mazur Yu. I., Ramsey K. A., Salamo G. J. Nanoscale Res Lett 2006, **1**, 57

[34] Gaudreau L., Saehrajda *et al.* Nature phys. 2012, **28**, 54

[35] Granger G., Gaudreau L. Phys. Rev. B 2010, **82**, 075304

[36] Yang C.-P., Chu S.-I., Han S. Phys. Rev. A 2003, **67**, 042311

[37] Amin M. H. S., Smirnov A. Yu., Maassen van den Brink A. Phys. Rev. B 2003, **67**, 100508(R)

[38] Nomoto K., Ugajin R., Suzuki T., Hase I., J. Appl. Phys. 1996, **79**, 291

[39] Tanamoto T Phys. Rev. A 2000, **61**, 022305

[40] Fedichkin L., Yanchenko M., Valiev K. A. Nanotechnology 2000, **11**, 387

[41] Hayashi T., Fujisawa T., Cheong H. D., Jeong Y. H., Hirayama Y. Phys. Rev. Lett. 2003, **91**, 226804

[42] Martinis J. M., Nam S., Aumentado J., Lang K. M. and Urbina C. Phys. Rev. B 2003, **67**, 094510

[43] Yoshihara F., Harrabi K., Niskanen A. O., Nakamura Y. and Tsai J. S. *Phys. Rev. Lett.* 2006, **97**, 167001

[44] Cywiński L., Lutchyn R. M., Nave C. P. and Sarma S. D. Phys. Rev. B 2008, **77**, 174509

[45] Kyriakidis J. *et al.* Phys. Rev. B 2002, **66**, 035320

[46] Ashoori R. C. *et al.* Phys. Rev. Lett. 1993, **71**, 613